Simulation Models of the Mark I Magnet and Dee

Author Mark1 AI instance, driven by Chris Mullins
Date 2026-09 **Revision** v0.2 (rev 1.2 models, revision note 2026-09-07)

Configuration magnet and dee as built 2017–2018 (gap 1.42 in), configuration continuous through 2025-02-02; models dated 2026-09-06

License CC BY 4.0

Machine at a glance

Type	Classical single-dee proton cyclotron, internal beam only
Magnet	H-frame, 1018 steel, 8 in poles, 1.42 in gap (as built); 538 turns of ¼ in copper refrigeration tubing, air-cooled
Field	0.851 T maximum at 55 A; operated at 570–596 mT in the beam era
RF	~9 MHz, ~50 W solid-state chain; dee voltage ~800 V nominal, uncalibrated
Chamber	304 stainless ring, ≈9.75 in bore, 1.000 in interior, ten KF16 ports, two 0.200 in lids
Best beam on record	−3.1 nA vs −0.55 nA background (5.6×), 596 mT / 9.033 MHz, 2023-10-14; ~150 keV-class computed
Built / operated	2017–2018 build; 176 logged runs on 44 dates, 2018-12-16 → 2025-02-02

1. Why publish the models

Every number in the other notes of this series that is not a measurement came from one of three places: the 2017 hand calculations, the 2018 FEMM design models, or the two new models built in 2026 for this series. Readers building a machine of this class can use the models directly: change a dimension, re-solve, and see what the change does before cutting steel. The models are small, free-software, and documented well enough to run from a clean install. They are also the honest way to publish the design method, because they show where the 2018 predictions were right, where they were right for the wrong reason, and what the field measurement can and cannot tell us.

Four packages are provided (Table 1). Each directory has its own README with the geometry, assumptions, run instructions and result tables; this note summarizes what they say.

Package	Tool	What it models	Solves	Regenerate in
`femm_2018`	FEMM 4.2, Lua	The original 2018–2020 design models, catalogued as found	—	seconds each

Package	Tool	What it models	Solves	Regenerate in
`femm_asbuilt`	FEMM 4.2, Lua	The same planar section rebuilt at as-built dimensions; current sweep and profiles	15	~1 min
`femm_es_dee`	FEMM 4.2 electrostatics	The dee between the lids: gap field, edge field, capacitance	4	~40 s
`elmer_hframe`	gmsh + Elmer 9.0	Full 3-D H-frame with round poles and ring coils, nonlinear 1018	8	~6 min

Table 1. The four downloadable packages. Solver outputs are not included; the scripts regenerate them.

2. The 2018 design models

The magnet was designed in FEMM 4.2 during 2018 with a hand-written Lua builder (`var_pole.lua` and its relatives) that draws the H-frame, poles, extensions and coils from a parameter list and solves a planar 2-D section. The section is the vertical mid-plane of the frame, extruded 8 in into the page, which is the width of the frame members and the diameter of the poles. Sweeps of coil current, pole gap, pole extension height and frame extensions were run from the same script; the workbook's B(I) "FEMM" column and the mid-plane radial profile used in the other notes come from these runs.

The catalogue in `femm_2018/README.md` describes each file. The main line is `mcm_2coil.FEM` (the two-coil model at the 1.50 in design gap) with `mcm.lua` for the current sweep and `mcm_2coil_gap_spread.lua` for the radial profile. Side studies were also kept: an air-core loop check (`hemholtz.lua`), the same coils with the iron replaced by air (`hemholtz2.lua`), and a comparison against a commercial magnet (`var_commercial.lua`). The last saved state of `var_pole.lua` is a different, recessed-pole study with 4 in poles and should not be mistaken for the Mark I geometry.

What the planar section cannot do is worth stating once. Square 8 × 8 in "poles" carry 27 % more flux than the real 8 in cylinders, so the yoke is loaded harder than in reality; the coils are straight bars rather than rings; and the pole-edge fringing is that of an infinite strip. The 2018 model was a trend tool at the 5 % level, and it did its job: it predicted saturation onset, the effect of pole extensions, and the field-versus-current curve well enough to size the supply.

3. The planar model at as-built dimensions

The 2018 script was cleaned into a single parametric file (`mk1_asbuilt.lua`, Lua 4.0) and re-run with the dimensions of the magnet as built: the measured 1.42 in gap instead of the 1.50 in design value, and the coil envelope the builder measured in September 2026: 6.0 in tall with a 5.0 in radial build on the 8.25 in form (about 18.25 in outside diameter; 269 turns at the 0.263 in sleeving pitch fill 62 % of that window, a hand-wound figure). The first release of this note used a 4.25 in packing estimate and 17 in OD; see the revision note at the end. Fifteen solves cover the current sweep, the profiles, and three variants.

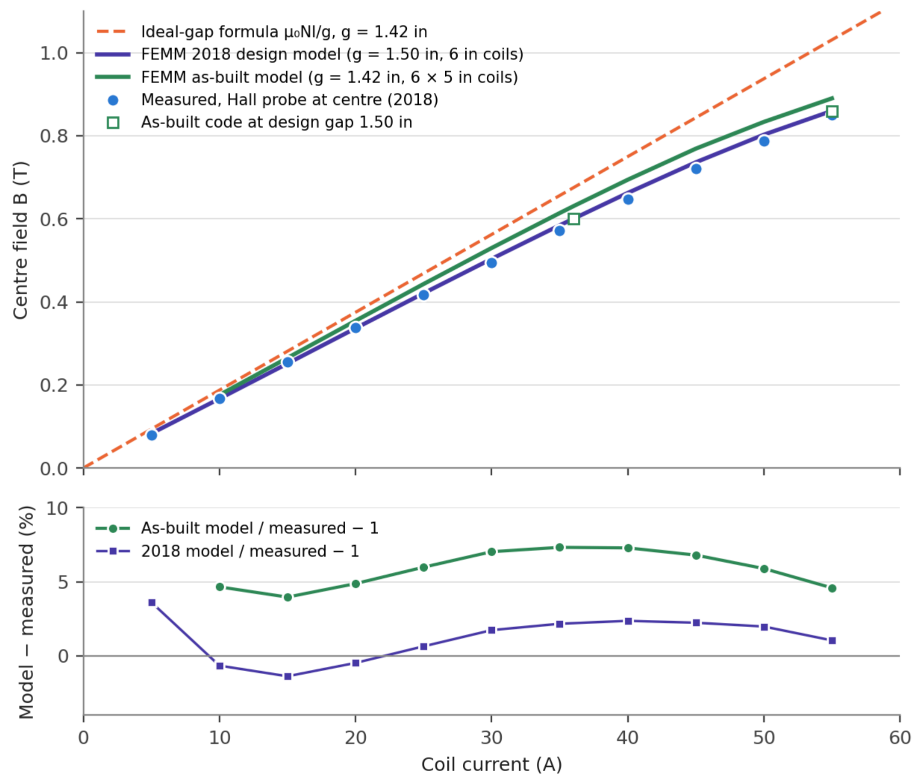

Figure 1. Center field vs coil current: ideal-gap formula, the 2018 design model (1.50 in gap), the as-built planar model (1.42 in gap), and the 2018 Hall-probe calibration. Lower panel: model minus measurement. The as-built model reads 4–7 % high at every current (4.7 % at 10 A, 4.6 % at 55 A); the 2018 model's 1–2 % agreement came from its too-wide design gap cancelling the model's optimism.

I (A)	As-built planar model (T)	Measured (T)	Model − measured	2018 model at 1.50 in (T)
10	0.176	0.168	+4.7 %	0.167
20	0.354	0.338	+4.8 %	0.336
30	0.529	0.495	+6.9 %	0.504
36	0.630	(beam-era band 0.570–0.596)	+5 to +10 %	—
40	0.693	0.647	+7.0 %	0.662
50	0.829	0.787	+5.3 %	0.803
55	0.890	0.851	+4.6 %	0.860

Table 2. Center field, planar model vs the 2018 Hall calibration. Same code at the design gap gives 0.858 T at 55 A. The design-to-built gap change is worth +3.6 % at 55 A and +5.0 % at 36 A (the bare gap ratio would be +5.6 %; iron reluctance dilutes it).

Three points follow. First, the over-prediction is already +4.6 % at 10 A, where nothing in the circuit is near saturation, so it is not a saturation-curve question; the real iron circuit loses more field at low excitation than FEMM's library 1018 curve does. Second, the shape of the error (rising to +7 % at 35–40 A, falling back to +4 % at 55 A) is the planar model's own yoke saturation pulling it down at high current: its square poles push 1.48 T through the side legs at 55 A. Third, joint reluctance is a percent-level effect: four 0.005 in air gaps in the pole circuit cost 1.0 % at 55 A. An area-matched variant (a 6.28 in pole width, which carries the true pole flux) unloads the yoke and gives 0.936 T at 55 A, so the planar model's own ambiguity spans 0.890–0.936 T.

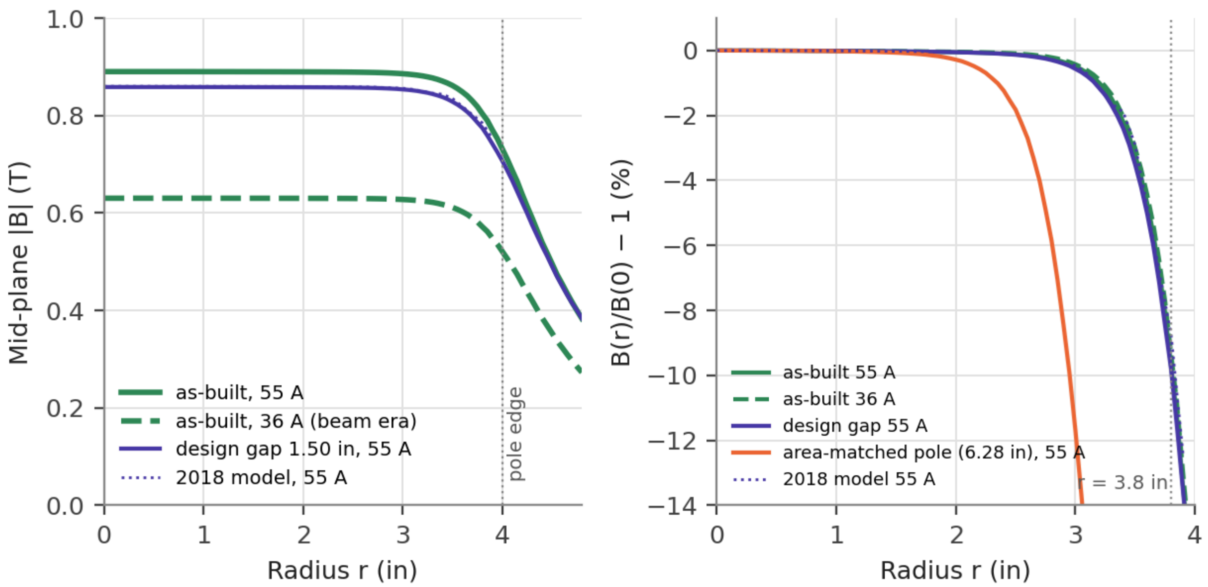

Figure 2. Mid-plane field along the radius (planar model). Left: absolute field at 55 A and at the 36 A beam-era point, with the design-gap and 2018 curves. Right: relative falloff. The field is flat to −0.5 % at the 3 in working radius and down 9.7 % at 3.8 in, where the collector sat for the best-beam runs. The area-matched variant, being a narrower strip, falls off much earlier and is shown only to mark the planar model's limits.

4. The 3-D model

The 3-D model (`elmer_hframe/`) reproduces the as-built magnet from the steel order and the construction spec: a 1018 H-frame of 3 × 8 in members, 8 in poles with 1 in extensions, the measured 1.42 in gap, and two 269-turn coils of 17 in outside diameter seated against the yoke faces. Meshed in gmsh (56,500 nodes, 341,000 tetrahedra, gap elements 5 mm) inside a 3 m air sphere, it is solved with Elmer's AV magnetodynamics solver with the iron as the same 1018 (B,H) table FEMM uses. Each nonlinear solve takes about five minutes on one core; the whole pipeline, mesh to figures, is about six minutes with the solves in parallel.

Item	As built	In the model
Frame	3 × 8 in 1018 members; top and bottom 28 in, sides 15.5 in	four boxes fused into one solid; corner joints perfect
Poles and extensions	8 in × 6 in plus 1 in extensions, bolted	one cylinder per side, yoke face to pole face; joints perfect

Item	As built	In the model
Gap	1.421 in measured at one point	1.42 in; aluminum chamber omitted
Coils	269 turns each, 6.0 in tall, 5.0 in radial build on 8.25 in forms (builder's measurement, Sept 2026)	annuli r = 4.0–9.125 in, 6.0 in tall, seated on the yokes, uniform current density, represented as their exact equivalent magnetization
Iron	cold-rolled 1018, actual curve unmeasured	FEMM library 1018 as a (B,H) table
Boundary	shop, steel cart 30 in below	A= 0 on a 3 m sphere; cart not modelled

Table 3. Geometry and assumptions of the 3-D model. The coil envelope is the builder's measurement; the first release inferred the 6.0 in height from photographs and solved a 4.6 in alternative (−1.6 % at 55 A), now historical.

Two controls on the same mesh anchor the numerics before any comparison with measurement: with ideal iron the center field at 10 A is 0.1873 T against NI/gap = 0.1874 T (−0.1 %), and with the iron removed the coil pair alone gives 11.05 mT against 11.08 mT from Biot–Savart (−0.3 %). Whatever disagreement remains with the probe is therefore a material-and-joint question, not a modelling error.

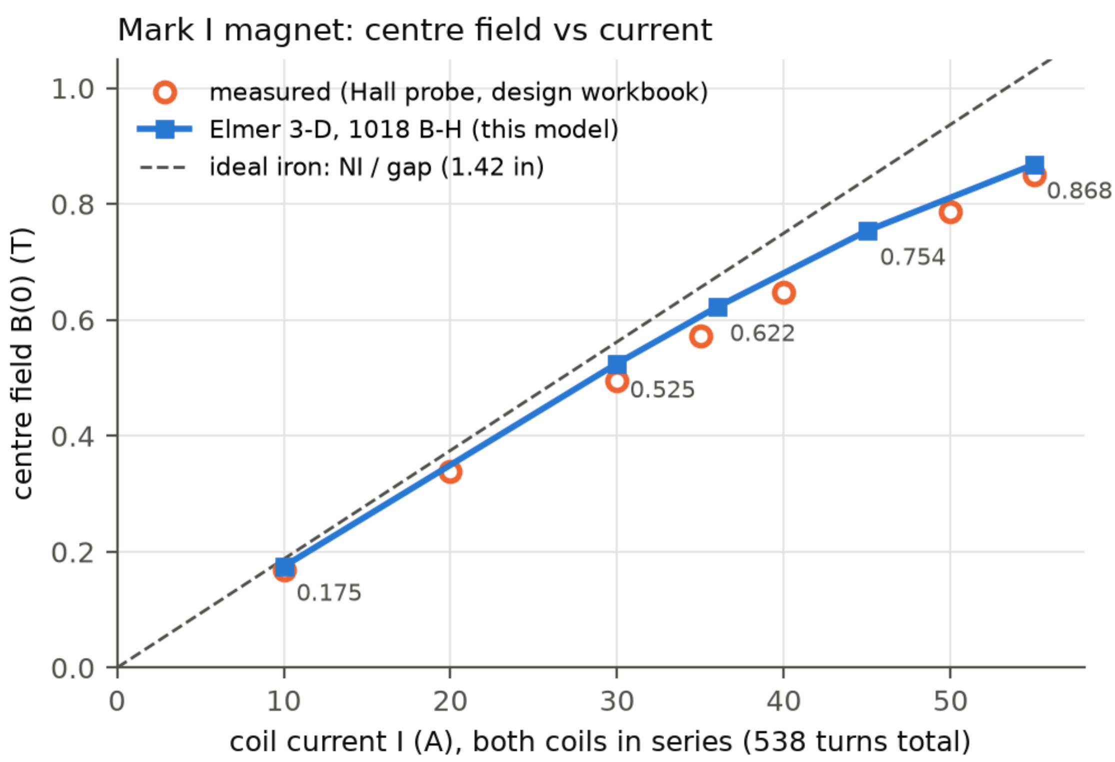

Figure 3. Center field vs current, 3-D model against the Hall calibration, with the ideal-iron line for reference. The model reads 2–6 % high; the excess is largest in the high-permeability range and shrinks at 55 A where the yoke enters the knee of the 1018 curve.

I (A)	Ideal iron NI/gap (T)	Elmer 3-D (T)	Measured (T)	Model − measured
10	0.187	0.175	0.168	+3.9 %
30	0.562	0.525	0.495	+6.1 %
36	0.675	0.623	(0.587 interpolated)	(+6.0 %)
45	0.844	0.754	0.720	+4.7 %
55	1.031	0.868	0.851	+2.0 %

Table 4. Center field, 3-D model vs measurement. Iron drop at 55 A is 16 % of the ideal value in the model; the frame's element-mean flux density is 1.41 T, the side members run at 1.09 T, and the pole-to-yoke corners reach 2.0–2.3 T.

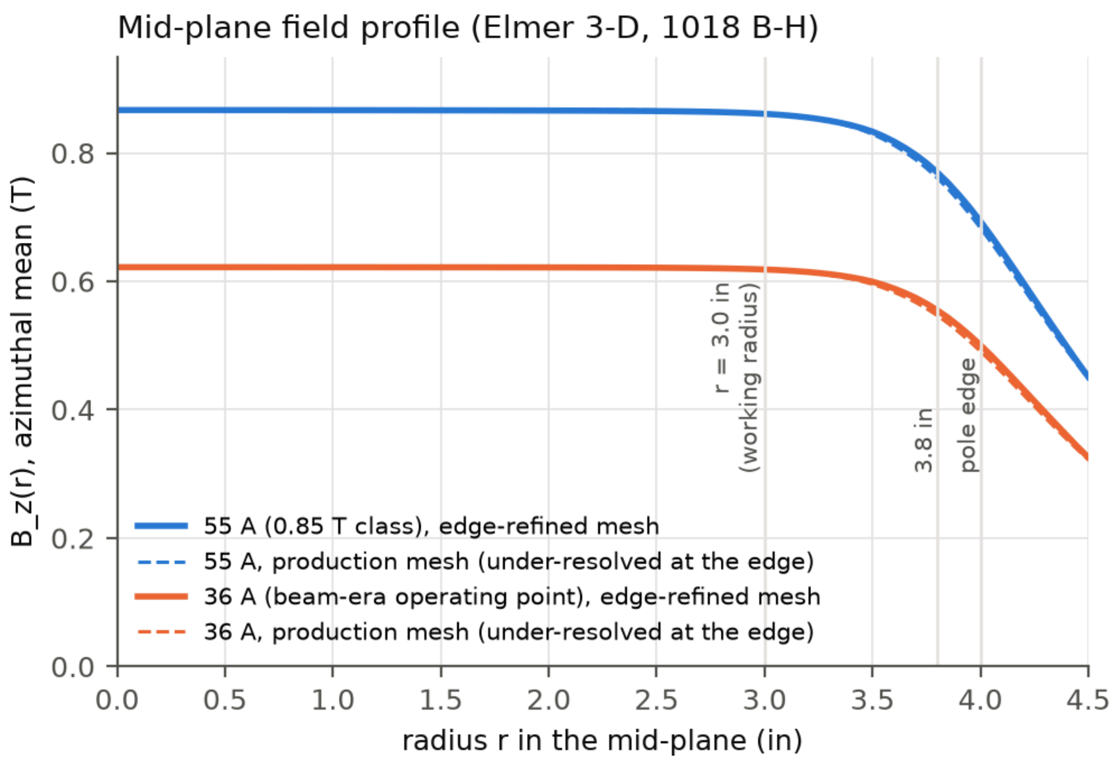

Figure 4. Mid-plane field profile from the 3-D model (azimuthal mean) at 55 A and at the 36 A beam-era point, on the edge-refined mesh (solid) and the production mesh (dashed). The field is flat to −0.8 % at r = 3.0 in; at 3.8 in, 0.2 in inside the pole edge, the refined mesh gives −10.7 % at 36 A and −11.1 % at 55 A (the production mesh, under-resolved there, gave −12.3 %), and B(4.0)/B(0) is about 0.79 at the pole edge.

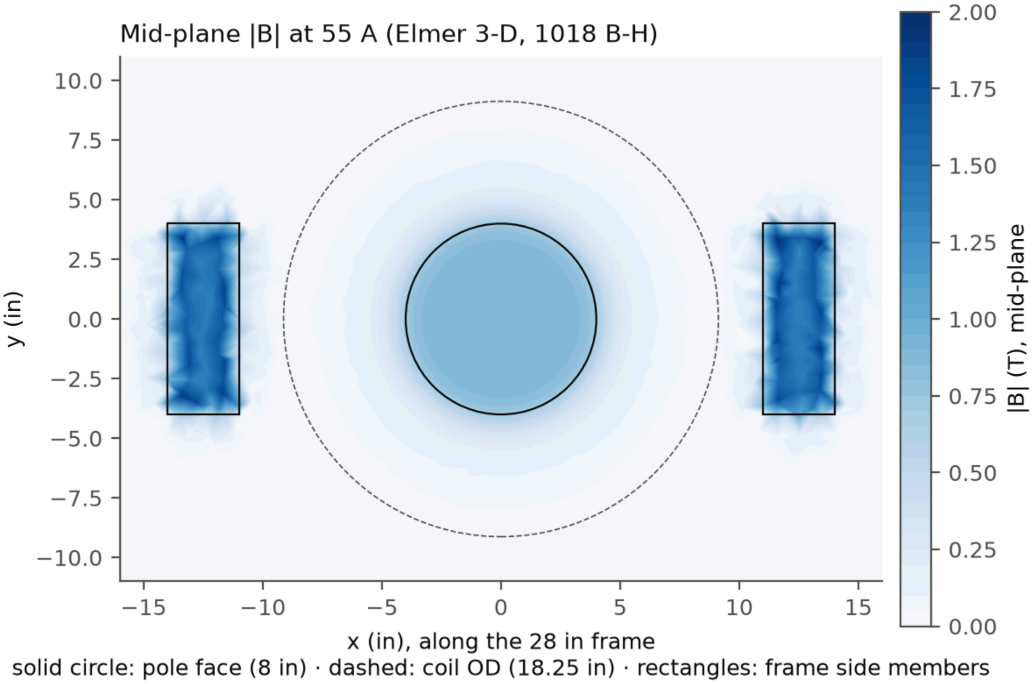

Figure 5. Flux density magnitude in the mid-plane at 55 A. The 8 in pole face carries 0.85–0.87 T; the two side members of the frame (rectangles) run at about 1.1 T with the corners approaching 2 T. The coil outline (dashed) is 17 in in diameter.

The external field is a number visitors ask about. One metre from the magnet center at 55 A the model gives about 160 µT (1.6 G) in the mid-plane and 315 µT (3.2 G) on the pole axis; at 36 A about 42 µT and 93 µT. These are ±20 % numbers (the boundary sits at 3 m and the elements at the 1 m probe are 0.11 m) and fall as $1/r^3$ beyond. A magnetically sensitive instrument on the bench sits in several times the Earth's field; nothing in the shop was affected in eight years of operation.

5. What the models say together about the measured field

Both models, one planar and one 3-D, read above the 2018 Hall calibration at every current, by 2–7 %, and both were checked against exact solutions on their own meshes. The 2018 design run's 1–2 % agreement is now understood as a cancellation between a 5.6 %-too-wide design gap and a model that runs a few percent optimistic. That is a common story with design models and worth telling plainly: agreement to 1 % from a 2-D trend model is a coincidence, not a calibration.

The shortfall the models leave to be explained is 2–6 % (3-D) or 5–7 % (planar), present already at 10 A. One caution before the list: the two models share the same library 1018 curve, so their agreement with each other says nothing about the leading suspect. Candidates, in the order a bench campaign would test them, cheapest first:

0. **The current and field instruments themselves.** A 3 % error in the supply's current readout would explain most of the gap on its own, and the Hall meter is a few-percent

instrument. Checking both against a reference ammeter and a reference probe costs an afternoon and no disassembly.

1. **The actual 1018 B–H curve.** Cold-rolled bar and plate from a steel supermarket vary in low-field permeability by heat and by cold-work state; neither model has a measured curve. This is the leading candidate because the excess is largest where the iron is far from saturation.
2. **Joint reluctance.** Eight steel-to-steel joints are in the circuit (frame corners, pole-to-yoke rod joints, extension shoulder-screw joints). The planar variant prices this at about 1 % per 0.020 in of cumulative air.
3. **Probe calibration.** The HT20 gaussmeter is a few-percent instrument; several meters and probes have been used over the years, none calibrated against a reference, and the probe is pushed into the gap blind, not quite reaching the pole center (see the instrumentation note).
4. **Gap geometry.** The gap was measured at one point (1.421 in) and not mapped for tilt or for the pole-extension seating.

A measured field map at two or three currents with a calibrated probe would settle most of this, and is the single most useful measurement the magnet has never had. It would also test the profile predictions of Figures 2 and 4, which matter to the energy convention used throughout this series: the log's computed energies assume the center field over the whole orbit, and the correction at the collector radius of 3.8 in is $(B(3.8)/B(0))^2$. The 2018 planar profile gives 0.90 for that ratio (energy × 0.82); the 3-D model on its edge-refined mesh gives 0.89 at the operating current (energy × 0.80), and its production mesh's 0.88 was a resolution artifact. For the 2023 best beam that is about 126–130 keV against the 158.7 keV uniform-field figure; the series quotes it as "~150 keV-class computed (158.7 uniform-field / ≈130 profile-corrected)", and the 3-D result is consistent with that.

6. The dee in its chamber (electrostatics)

The dee is a hollow half-pillbox: two 4 in-radius half-discs of 3/32 in aluminum sheet on a 0.5 in tall curved rim ring, 0.69 in tall overall, with the straight (accelerating) edge open, so the ions pass through a mouth between two sheet lips into the field-free interior. It sits on loose Viton pieces between two grounded lids 1.000 in apart, with a nominal 0.155 in clearance above and below. There is no dummy dee: the far side of the accelerating gap is the grounded lids and chamber wall. Two FEMM electrostatic sections were solved at 800 V: a planar section through the machine center perpendicular to the straight edge, with the vacuum inside the dee meshed and the lips rounded to half the sheet thickness (the real tin-snipped lips are irregular), and an axisymmetric full-disc model for the curved rim. Sensitivity cases cover mesh refinement, the lids bowed inward under vacuum by the measured 33 mil, and a 0.05 in sag of the free-floating dee. (The first release of this note modelled the dee as a closed conducting block, which seals the mouth; see the revision note.)

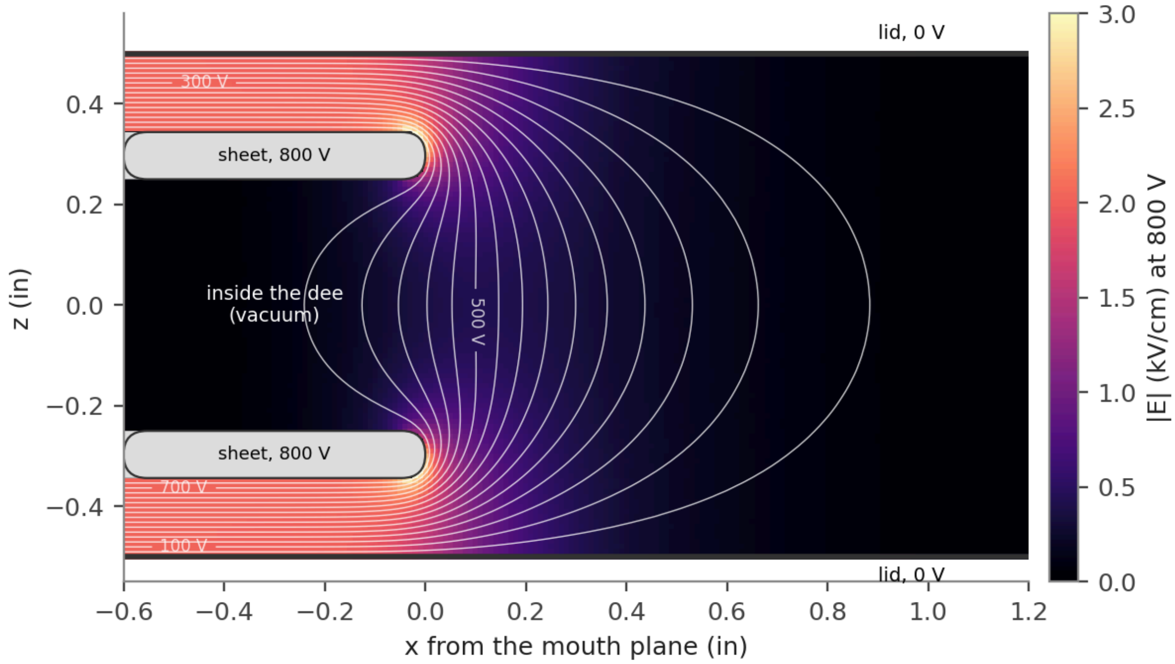

Figure 6. Field magnitude and equipotentials around the open mouth of the dee at 800 V (planar section, vertical scale exaggerated by the aspect ratio). The strong field is in the 0.155 in lid gaps above and below the sheets; the potential penetrates into the hollow dee, and the accelerating region outside the mouth is soft and about three-quarters of an inch long.

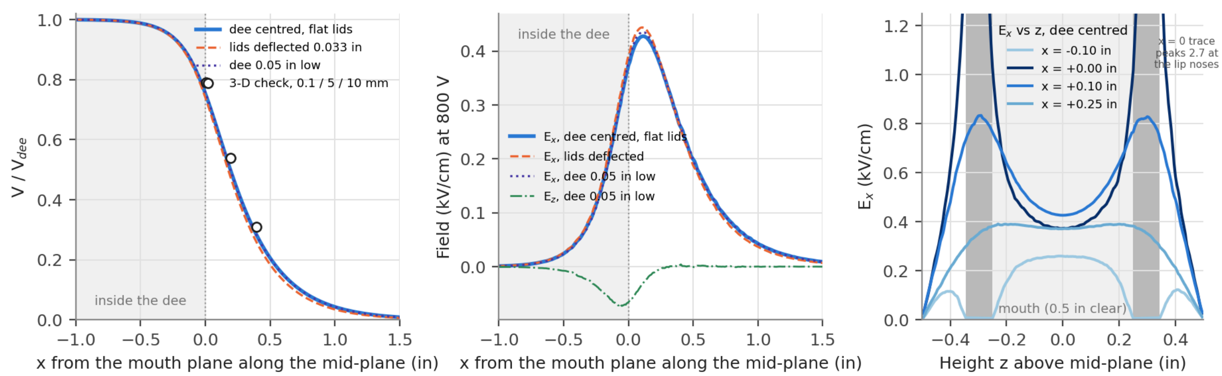

Figure 7. Left: potential and accelerating field along the mid-plane from inside the dee through the mouth and outward; a quarter of the dee voltage is already gained inside the mouth, and the field peaks about 0.1 in outside it. Right: the accelerating field across the chamber height at the mouth plane and just outside it, flat only over the central ±0.1 in and rising toward the lips.

Quantity	Result at 800 V	Note
Potential at the mouth plane	0.75 × dee voltage	the ion gains a quarter of the voltage inside the dee; agrees with an independent 3-D solve (0.78–0.79) to a few percent
Mid-plane accelerating field	0.37 kV/cm at the mouth; peak 0.43 kV/cm 0.115 in outside it	a fifth of the lid-gap field V/g = 2.03 kV/cm

Quantity	Result at 800 V	Note
Effective gap length ∫E dx / E_max	0.74 in (19 mm)	10–90 % of the voltage is gained over 0.90 in
Field uniformity across the mouth	within 10 % over the central ±0.10 in	1.6× higher within 0.05 in of the lips
Peak surface field, lip (3/64 in radius)	3.3 kV/cm (converged to 0.3 %)	3.9 with the lids bowed; 4.3 with the dee 0.05 in low; 21 / 54 kV/cm at a 5 / 13 kV dee
Dee-body capacitance, flat lids	84 pF	faces 72.9 + curved-rim fringe 7.1 + straight-edge fringe 3.8; the closed-body model gave 84.4
Design workbook derivation	74.35 pF	edge term about half the real fringing; 0.160 in gaps instead of 0.155
Lids deflected under vacuum (33 mil at center, measured)	≈ 93 pF body	the mean dee-to-lid gap shrinks from 0.155 to about 0.137 in; face term × 1.13
Measured (2018, in place)	100 pF	the remainder is stem, feedthrough and wiring: ~7 pF if measured under vacuum, ~16 pF if at atmosphere; the record gives neither the pressure state nor the measuring circuit
Dee sagging 0.05 in	C +10.5 % (≈93 pF at atmosphere); mid-plane vertical field 0.07 kV/cm at the mouth	resonance moves ~5 %; the accelerating field is barely changed

Table 5. Electrostatic results for the open-mouth dee. All fields scale linearly with the real dee voltage, which was never measured.

Three consequences are worth drawing out. The 74 → 100 pF discrepancy in the 2018 tuning record, never reconciled in the workbook, is mostly explained: the workbook under-counted fringing (74 vs 84 pF), and under vacuum the lids bow 33 mil inward so the dee body itself is about 93 pF, leaving only a few picofarads for the stem and feedthrough the workbook never modelled, or about 16 pF if the 100 pF was measured with the chamber at atmosphere. A ~6 % resonance shift between the two states is the arbiter, and no feedthrough capacitance should be inferred by subtraction until the measuring circuit is known. The free-floating dee's position moves the tank capacitance by more than 10 % for a 0.05 in sag, a plausible contributor to the day-to-day retuning the log records. And the accelerating gap without a dummy dee is a soft region about 19 mm long rather than a defined gap: a quarter of the dee voltage is gained inside the mouth and the rest over the next three-quarters of an inch, a distance that a 30 keV proton covers in about 31° of RF phase at 9 MHz and a 1 keV first-turn ion in well over a full cycle. That transit-time effect is one reason the first turns are where a machine of this class loses beam, and it is the argument for a dummy dee or a defined ground electrode in any successor.

7. Running the models

FEMM (Windows, free): install FEMM 4.2; from a shell, femm.exe -lua-script=<path>\mk1_asbuilt.lua -windowhide runs a sweep headless and writes CSV results next to the script. The Lua dialect is 4.0 (no ipairs, getn for lengths, .. for strings). The package includes a small wrapper that starts a dialog watcher, since a modal error under -windowhide is invisible and stalls the run. Each magnetostatic solve takes 2–3 s; the electrostatic cases 5–15 s.

Elmer (Windows or Linux, free): the pipeline is gen_mk1_mesh.py (gmsh Python SDK, millimetres, physical groups per body) → ElmerGrid 14 2 mk1.msh -autoclean -scale 0.001 0.001 0.001 → make_mk1_sif.py <current> → ElmerSolver → post_mk1.py for tables and figures. run_mk1.sh does all of it. Conventions that cost real time to learn are in the README: Elmer's H–B curve table is in (B, H) order; every physical volume needs a Body section; windings are represented as their equivalent magnetization; the AV solver converges with plain CG and no preconditioner.

8. Limitations and the measurements that would close them

- **No measured field map.** Every profile here is a prediction. A mid-plane map at 20, 36 and 55 A with a calibrated probe (radial to the pole edge, at four azimuths) is the priority measurement.
- **Mesh convergence** is established for the center field (~0.2 %) and, after local pole-edge refinement, for the mid-plane profile to about ±0.2 points at 3.8 in; local vector accuracy near the pole edge, which a tracking study would need, is not.
- **No measured B–H curve** for the actual bar stock, and no joint characterization. A coil-current versus center-field curve at low current (2–10 A) with the same probe would separate permeability from joints.
- **Coil envelope** is now the builder's measurement (6 × 5 in); the winding's internal layout (62 % fill, hand-wound) is still idealized as uniform current density. The coil resistance would pin the copper length.
- **The dee model assumes a flat, centered sheet** with a uniform 3/32 in edge radius. The real edge is tin-snip wavy and the dee's position varies; an LCR measurement of the dee in place (expected ~84 pF body, ~100 pF with stem) would test the capacitance accounting directly.
- **Hysteresis and remanence** (a ≈1.4 A-wide loop, 16–19 mT remanence in the workbook) put ±1–2 % on any single calibration point and are not modelled.

Revision note (rev 1.2, 2026-09-07)

Four corrections to the first release of this note (2026-09-06). Two came from the builder's measurements; two were found by an independent verification campaign on the same models (Mark I modeling, Sept 2026), which re-solved the published packages with its own meshes, controls and acceptance targets. The corrected model packages carry the same revision.

Magnet coil geometry (builder). The first release described the coils as 17 in OD and, in the planar model, 4.25 in tall by a packing estimate; the 3-D model used 6.0 in from photographs. The builder measured the coils on 2026-09-07: each is 6.0 in tall with a 5.0 in radial build on the 8.25 in form, about 18.25 in OD, with 269 turns filling 62 % of the window. Both models were re-solved at the measured envelope. The center field barely moves (planar +0.06 % at 10 A to +0.6 % at 55 A, 3-D −0.03 % to −0.25 %), confirming that the field is set by NI and the iron circuit while the coil envelope only redistributes leakage. Every model-versus-measurement conclusion stands.

Outer boundary of the 3-D model and the pole-edge profile (verification campaign). The first release's 3-D mesh had no boundary elements on its 3 m sphere: the script selected the outer surface by a test that could never succeed, so the A = 0 condition was never applied and the solver worked on a singular system. The campaign found this by reading the mesh file. Applying the condition changes the center field by less than 0.006 % and none of the B(I) conclusions, but the 1 m stray field by 5–14 %; the stray-field figures in §4 are now from the corrected model. The campaign also showed that the mid-plane profile at 3.8 in is under-resolved on the production mesh: with local refinement at the pole edge, B(3.8 in)/B(0) settles at about 0.89 (−11 %) rather than the 0.88 (−12.3 %) first reported. The package now carries the edge-refined mesh as an option, solved at 36 and 55 A: B(3.8 in)/B(0) = 0.892 and 0.888, i.e. −10.7 % at the operating point and −11.1 % at full current, ±0.2 points, with the center field converged to about 0.2 %. The same campaign showed that the first release's suggestion that ~0.1 mm of series air at the joints would close the low-current discrepancy was wrong by an order of magnitude (about 1.5 mm equivalent would be needed), so the joints are unlikely to be the whole story. The consequence for the energy convention in §5 is that the profile-corrected best beam moves back to about 126 keV, in line with the ≈130 keV the run history carried, and the first release's statement that the 3-D model favored the low end of the range was a mesh artifact.

Open-mouth dee (verification campaign). The first release modelled the dee as a closed conducting block, which seals the accelerating edge with a conductor; the real dee is hollow with an open mouth between two sheet lips. A 3-D check gave a potential of about 0.79 of the dee voltage just outside the mouth versus 0.99 for the closed body, with the capacitance nearly unchanged. The package now models the open mouth; §6 and Table 5 carry the corrected results: the field peaks 0.1 in outside the mouth at 0.43 kV/cm (not 0.68 at a face), the effective gap is 0.74 in (not 0.46), the field across the mouth is flat only over the central ±0.1 in, and the peak surface field is 3.3 kV/cm on the lips. The capacitance accounting changes by under 1 %. The closed-body numbers are kept in the package README as a marked historical table.

Deflected-lid capacitance (this revision, prompted by review). The first release's capacitance accounting (workbook 74 pF → modelled body 84 pF → measured 100 pF, leaving ~16 pF to stem, feedthrough and wiring) used flat lids. Under vacuum the 0.200 in lids bow inward a measured 33 mil at center, and the dee sits under that center. With both lids so deflected, the face term scales by about 1.13 averaged over the half-disc, so the dee body under vacuum is about 93 pF and the unexplained remainder is about 7 pF, not 16, if the 100 pF was measured with the chamber pumped down. The record gives neither the pressure state nor the measuring circuit of that 100 pF, so no feedthrough capacitance is claimed by subtraction.

Sources

Design workbook `cyclotron9.xlsx` (sheets `sim`, `Specs`, `iron`, `RF matching`, `magnet time constant`); the 2018 FEMM models and Lua scripts; construction spec and steel order (frame and pole dimensions); build website photographs of the coils (2018) and the 2024 teardown photographs (coil seating); the run log; the builder's review, Aug 2026 (gap, coil construction, dee construction). Model packages and their READMEs: `femm_2018`, `femm_asbuilt`, `femm_es_dee`, `elmer_hframe` (2026-09-06). Toolchain: FEMM 4.2, gmsh 4.15, Elmer 9.0.
